

# Computer Simulation Studies of Static and Dynamical Scaling in Dilute Solutions of Excluded-Volume Polymers

Anthony J. C. Ladd\*

Lawrence Livermore National Laboratory, University of California, P.O. Box 808, Livermore, California 94550

Daan Frenkel

FOM Institute for Atomic and Molecular Physics, Kruislaan 407, 1098 SJ Amsterdam, The Netherlands

Received November 18, 1991; Revised Manuscript Received March 17, 1992

**ABSTRACT:** We have used a novel Monte Carlo method to compute the gyration radius  $R_G$  and the hydrodynamic radius  $R_H$  of excluded-volume polymer chains. The hydrodynamic radius scales as  $N^{0.55}$  ( $N$  is the number of bonds) over at least a decade of chain lengths, whereas the gyration radius exponent is close to the theoretical value of 0.59. The anomalous behavior of  $R_H$  is well-known experimentally; it is commonly attributed to the belief that polymers in mediocre solvents are not swollen on short length scales. However, the polymer chains in our simulations are uniformly swollen on all length scales; we suggest that the discreteness of the polymer chain is sufficient to explain the behavior of  $R_H$ .

The effective size of a polymer chain scales as a power  $\nu$  of the molecular weight.<sup>1,2</sup> Static measurements of the radius of gyration of a dilute polymer solution in a good solvent give an exponent  $\nu_G = 0.595 \pm 0.005$ ,<sup>3</sup> close to the renormalization theory result for a self-avoiding random walk,  $\nu = 0.588$ .<sup>4</sup> Dynamical measurements of diffusion or viscosity coefficients indicate a smaller exponent  $\nu_H \approx 0.55$ .<sup>5,6</sup> It was suggested initially that the dynamic and static scaling laws are different, but this idea has been generally discarded in favor of arguments based on solvent effects. For a general discussion of the scaling of  $R_G$  and  $R_H$ , see refs 1 and 2. Weill and des Cloizeaux<sup>7</sup> suggested that in mediocre solvents only large segments of the chain, containing many statistical units (bonds), are swollen; the smaller length segments are ideal; that is, their size scales as the square root of the number of bonds. Thus the observed exponent for a finite length chain will be somewhere between ideal ( $\nu = 1/2$ ) and swollen ( $\nu = 0.588$ ); since the hydrodynamic radius weights the short distances more heavily than the gyration radius, its effective exponent will be smaller. In this work we have used a powerful new Monte Carlo technique, configurational-bias Monte Carlo (CBMC), to examine the connection between the swelling of internal segments of long polymer chains and the hydrodynamic and gyration radii of those chains.

Our polymer model is a freely-jointed chain with a unit bond length between the joints; the excluded volume is introduced by placing rigid spheres of diameter  $\sigma$  ( $0 \leq \sigma \leq 1$ ) at each joint. Single chains containing between 2 and 1025 spheres were simulated, with 1000 independent chain configurations for each reported result; the statistical errors in the gyration and hydrodynamic radii are then small (0.5%). In order to efficiently generate many statistically independent chain conformations, we employed the recently developed configurational-bias Monte Carlo scheme for fully flexible molecules.<sup>8</sup> The basic Monte Carlo step in this scheme is a partial (or total) regrowth of the chain; the chain is cut at some randomly selected point and regrown from there. Of course, a random regrowth of the polymer would almost certainly result in a self-overlapping (forbidden) conformation. For polymers on a lattice, this problem can be alleviated by regrowing the polymer using a biased procedure due to the Rosenbluths.<sup>9</sup> In this

procedure the polymer is not regrown randomly; rather, at every step it only moves in one of the  $k$  directions (out of a maximum of  $b$ ) that are not yet occupied. Due to the bias in the growth process, the conformations are not generated with the correct statistical weight; to compensate for this bias, Rosenbluth and Rosenbluth introduced a weight factor  $w$ , defined as

$$w = \prod_{i=1}^l (k_i/b) \quad (1)$$

for a trial chain of  $l$  segments. In ref 9 it is shown that this factor  $w$  should be used as a weighting factor in any statistical average over chain conformations generated using the Rosenbluth prescription. Unfortunately, for long chains this procedure is unreliable because the probability of generating chains with a large "Rosenbluth weight" becomes very small. Recently, it was shown that this drawback of the original Rosenbluth scheme can be overcome by using a Monte Carlo scheme in which the acceptance probability of a trial conformation is proportional to the ratio of the Rosenbluth weights of the new and old conformations  $w^{\text{trial}}/w^{\text{old}}$ ,<sup>10</sup> a less general version of this scheme was presented earlier.<sup>11</sup> We shall refer to this method as the configurational-bias Monte Carlo method. Still, the CBMC method as described in ref 10 is limited to molecules with discrete conformations; recently however, Frenkel et al. showed how the CBMC method can be extended rigorously to fully flexible molecules.<sup>8</sup> In this case, the number of possible trial directions  $b$  at any step is, in principle, infinite. However, it is shown in ref 8 that a correct Monte Carlo procedure can be devised by generating a random subset of this infinity of possible trial directions and computing the Rosenbluth weight  $w$  for this finite subset. It should be stressed that the validity of this scheme in no way relies on the number of trial directions in this subset; in fact, one could generate only one trial direction per step, in which case the conventional, random-walk sampling would be recovered. The actual number of trial directions is chosen to optimize the computational efficiency of the scheme; typically the number of trial directions varies from 2 to 3 for short chains, to 50 if long chains are regrown. For more details about the CBMC method, the reader is referred to refs 8 and 12.

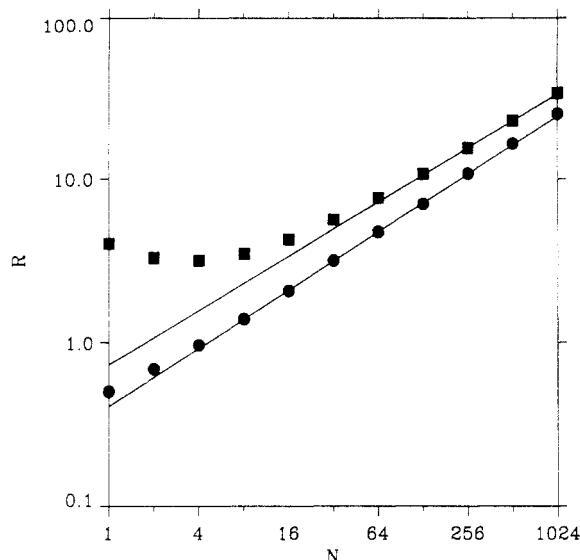


**Figure 1.** Gyration radii (circles) and inverse radii (squares) of excluded-volume chains as a function of the number of bonds  $N$ . For clarity, the inverse radius is shown multiplied by 2. The straight lines are power-law fits  $R \propto N^\nu$  to the simulation data; the exponents are  $\nu_G = 0.59$  and  $\nu_H = 0.55$ , for the gyration and hydrodynamic radii, respectively.

Although in the present work we consider isolated, linear, fully flexible homopolymers, it should be stressed that the CBMC method is very versatile and is no way limited to any of these four categories. In our simulations, we do however exploit the fact that we are dealing with linear homopolymers, by allowing a partial regrowth to take place at either end of the chain. If only one segment is regrown, our CBMC scheme reduces to the well-known (but slow) reptation scheme.<sup>13</sup> We find that the acceptance ratio for a complete chain regrowth step is about 2% in the worst case ( $\sigma = 1$ ,  $N = 1024$ ). In practice, we perform many (partial) chain regrowths between two samplings of the structural properties of the polymer: for the largest spheres ( $\sigma = 1$ ), independent configurations of an  $N$ -bond chain require about  $N$  regrowth steps; for smaller spheres  $\sigma N$  steps were used.

The gyration radius and inverse radius of an  $N$ -bond bead polymer can be written in terms of the distance  $R_{ij}$  between beads  $i$  and  $j$ .

$$R_G^2 = \frac{1}{(N+1)^2} \left\langle \sum_{i>j} R_{ij}^2 \right\rangle, \quad R_I^{-1} = \frac{2}{(N+1)^2} \left\langle \sum_{i>j} R_{ij}^{-1} \right\rangle \quad (2)$$

The inverse radius  $R_I$  is closely related to the hydrodynamic radius  $R_H$ ,<sup>1,2</sup> defined as the radius of the hydrodynamically equivalent sphere

$$R_H = \frac{k_B T}{6\pi\eta D} \quad (3)$$

where  $D$  is the diffusion coefficient at infinite dilution. In comparison with experimental results, we will assume that, for sufficiently long chains, the hydrodynamic radius  $R_H$  and the inverse radius  $R_I$  have the same scaling with chain length; other estimates of  $R_H$  will be examined at the end of the paper.

In these simulations we do not account for the solvent explicitly; rather, by varying the size of the excluded-volume sphere, we model varying solvent conditions, from athermal ( $\sigma \approx 1$ ) to the  $\Theta$  point ( $\sigma \approx 0$ ) where the chain statistics are nearly ideal. The results quoted in the present paper will be for chains of spheres with diameter  $\sigma = 0.65$  since this model closely approximates the conformational properties of polystyrene in good solvents such

as benzene or toluene, as can be seen as follows. First we account for chain stiffness in the usual way, by assigning several monomer units to one statistical unit or bead of our polymer chain. From the model parameters given by Yamakawa,<sup>14</sup> we can estimate the contour length of the chain  $L$  as a function of molecular weight. Then, by comparing the radius of gyration at the  $\Theta$  temperature,<sup>5</sup> with that for an ideal chain ( $R_G^2(\Theta) = L^2/6N$ ), we can estimate the number of statistical units in the chain. We find about 10 monomers, or a molecular weight of about 1000, per statistical unit. Thus our longest chain, containing 1025 spheres, corresponds to a molecular weight of about  $10^6$ ; light-scattering measurements of the hydrodynamic radius of polystyrene solutions range over molecular weights from  $10^4$  to  $10^7$ .<sup>6</sup> With the assumption that there are 10 styrene monomers per statistical unit, we can determine the appropriate size of the excluded-volume sphere by comparing the swelling factors  $\alpha = R_G/R_G(\Theta)$ . Experimentally,  $\alpha$  can be determined by comparing the radius of gyration of polystyrene in a good solvent such as benzene or toluene with that in a  $\Theta$  solvent like cyclohexane. In the simulations, we compare the radius of gyration as a function of  $\sigma$  with that for an ideal chain. We find that for  $\sigma = 0.65$  the swelling factors are within 5% of those for polystyrene in room-temperature benzene or toluene.<sup>5,6</sup>

In Figure 1 we plot the gyration radius and the inverse radius vs the logarithm of the number of bonds for  $\sigma = 0.65$ . In the case of the radius of gyration the asymptotic scaling  $R_G \propto N^{0.59}$  is obeyed almost perfectly for  $N > 4$ . However, for the inverse radius the apparent asymptotic exponent is 0.55, exactly the same as the experimental result; but this is *not* due to a transition from unswollen to swollen segments, as can be seen in Figure 2. Here we plot the average size of a segment of contour length  $n$  within a chain of 1024 bonds vs the logarithm of  $n$ ; we define two different sizes based on square and inverse distances

$$R_G(n)^2 = \frac{1}{(N+1-n)} \left\langle \sum_{i>j=n} R_{ij}^2 \right\rangle, \quad R_I(n)^{-1} = \frac{1}{(N+1-n)} \left\langle \sum_{i>j=n} R_{ij}^{-1} \right\rangle \quad (4)$$

Apart from end effects, which we discuss below, we find  $R(n)$  scales as  $n^{0.59}$  over almost the whole range of  $n$  for both  $R_G(n)$  and  $R_I(n)$ ; i.e.

$$R(n) = A n^{0.59} \quad (5)$$

The solid lines in Figure 2, with  $A_G = 1.1$  and  $A_I = 0.9$ , show that  $R_G(n)$  and  $R_I(n)$  fit this functional form very well for  $n > 4$ . Similar studies with different length chains show that  $R_G(n)$  and  $R_I(n)$  are essentially universal functions of  $n$ , regardless of the length of the chain, provided  $N > n + 2$ . Deviations from the universal behavior are typically on the order of 1%, 4%, and 10% for  $n = N - 2$ ,  $n = N - 1$ , and  $n = N$  (the end-to-end distance), respectively. This is in good agreement with experiments measuring internal chain sizes of deuterium-labeled polystyrene,<sup>15</sup> which show that the internal segments are more swollen than a comparable length chain; our simulations show that when referred to a universal swelling function, it is the end-to-end distance that is less swollen, rather than the internal segments being more swollen. Thus our simulations show that the chain is more or less uniformly swollen (apart from end effects), with the expected asymptotic exponent of a self-avoiding random walk. Moreover, at short length scales the effective

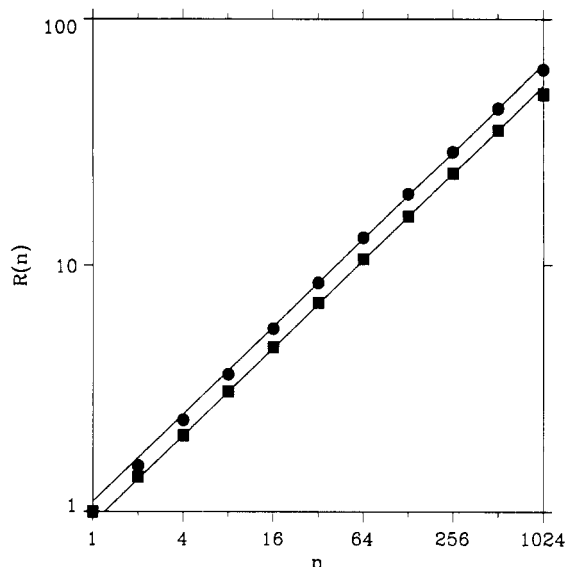


**Figure 2.** Segment-size scaling of a 1024-bond excluded-volume chain as a function of the segment length  $n$ . The average values of  $\langle R_{ij}^2 \rangle^{1/2}$  (circles) and  $\langle R_{ij}^{-1} \rangle^{-1}$  (squares) are shown for all pairs of beads  $i > j$  with  $i - j = n$ . The straight lines are power-law fits  $R \propto n^\nu$  to the simulation data; the exponents are  $\nu = 0.59$  in both cases. The last point  $n = 1024$  is noticeably perturbed by end effects.

exponent of  $R_G(n)$  is, if anything, larger than 0.59. In other words, we do not observe ideal chain statistics ( $\nu = 0.5$ ) at any length scale. Weill and des Cloizeaux's theory<sup>7</sup> is based on the blob model, in which the short length segments (blobs) exhibit ideal scaling, and only segments larger than some critical size are swollen. In order to account for a nonasymptotic exponent  $\nu_H = 0.55$  in the experimental molecular weight range, Weill and des Cloizeaux assume that the blob size is about 200 monomers for polystyrene in benzene or about 20 statistical units; other estimates of blob size in room-temperature benzene and toluene range from 5 to 12.<sup>5</sup> Our simulation results do not support the assumption of ideal chain statistics in this region, but nevertheless, the exponent characterizing the inverse radius has not reached its limiting value.

In order to understand the simulation results, we first note that the gyration and inverse radii can be expressed exactly as properly weighted sums over the  $R(n)$ 's

$$R_G^2 = \frac{1}{(N+1)^2} \sum_{n=1}^N (N+1-n) R_G^2(n),$$

$$R_I^{-1} = \frac{2}{(N+1)^2} \sum_{n=1}^N (N+1-n) R_I^{-1}(n) \quad (6)$$

Assuming  $R_H = R_I$  (eq 8), we can estimate the hydrodynamic radius for each  $N$  from eqs 5 and 6 and extrapolate beyond the range of the simulation data; the results are shown in Figure 3. It can be seen that the agreement with the simulation data for  $R_I$  is excellent; even the unusual minimum in  $R_I$ , due to the neglect of monomer friction, is accurately reproduced. The main point is that the exponent characterizing the hydrodynamic radius is converging very slowly to its asymptotic value, even though the internal segment lengths obey the asymptotic scaling  $R(n) = n^{0.59}$ . According to our model, polystyrene polymers with molecular weights on the order of  $10^8$  would be necessary to observe the asymptotic exponent clearly, whereas the experimental molecular weight range is between  $10^4$  and  $10^7$ . The reason for the slow convergence of the exponent has been discussed by Guttman,<sup>16</sup> who pointed out that higher order corrections to the asymptotic

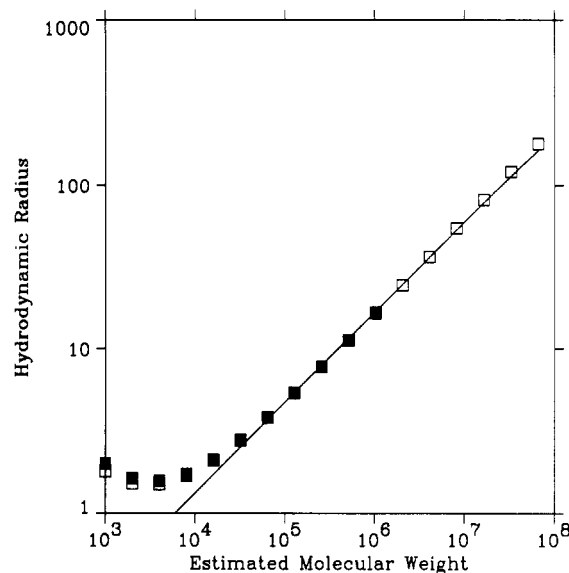


**Figure 3.** Estimated scaling of the hydrodynamic radius for polystyrene in good solvent, based on a molecular weight of 1000 per statistical unit (bead). The solid squares are the simulation data as in Figure 1, and the open squares are computed from eqs 5 and 6, with  $A = 0.90$ . The straight line is a power-law fit with an exponent of  $\nu = 0.55$ . The asymptotic value of the exponent  $\nu = 0.59$  is not reached, in this model, until molecular weights on the order of  $10^8$ .

scaling are likely to be noninteger powers of  $N$ . In fact, from eqs 5 and 6, using  $A_I = 0.9$  (Figure 2), we find for large  $N$

$$R_I^{-1} = 3.84N^{-0.59} - 4.08N^{-1} \quad (7)$$

In Figure 3 we see that the experimental molecular weight range ( $10^4$ – $10^7$ ) is characterized by an effective exponent  $\nu_H = 0.55$  (again assuming that the molecular weight of a statistical unit is 1000). Thus the static/dynamic exponent anomaly can possibly be explained by discrete chain effects which, because of the large weight given to short distances, have a surprisingly significant effect on the hydrodynamic radius; another factor is the chain stiffness which increases the size of the statistical units from 1 to about 10 monomers.

Finally, we have also computed the Kirkwood and Zimm approximations to the hydrodynamic radius. In the Kirkwood approximation, the drag force on each bead is assumed to be equal to the gravitational force; a contribution from the monomer friction is included, so that

$$R_K^{-1} = [(N+1)a_H]^{-1} + R_I^{-1} \quad (8)$$

where  $a_H$  is the hydrodynamic radius of the statistical unit. For asymptotically long chains, the contribution from monomer friction is negligible; thus  $R_K$  is equivalent to  $R_I$  in this limit. In the Zimm approximation,<sup>17</sup> the polymer is assumed to be a rigid body, with fluctuating, configuration-dependent drag forces on the individual beads; to solve it requires an inversion of the hydrodynamic matrix. The Zimm approximation has been used to calculate the hydrodynamic radius of excluded-volume chains,<sup>18</sup> but the maximum chain length ( $N = 54$ ) was much shorter than in our work. Fixman<sup>19</sup> has shown that  $R_K$  is a lower bound to the true hydrodynamic radius  $R_H$  and that  $R_Z$  is an upper bound to  $R_H$ ; typically they differ by about 10%. Dynamical simulations on short Gaussian chains ( $N \leq 55$ )<sup>20</sup> indicated that the hydrodynamic radius lies approximately halfway between the two bounds. We have computed  $R_K$  and  $R_Z$  assuming Rotne-Prager hydrodynamic interactions<sup>21</sup> and a hydrodynamic radius of the beads equal to the collision radius ( $a_H = 0.325$ ); the results are shown in Figure 4 and are also collected in Table I for

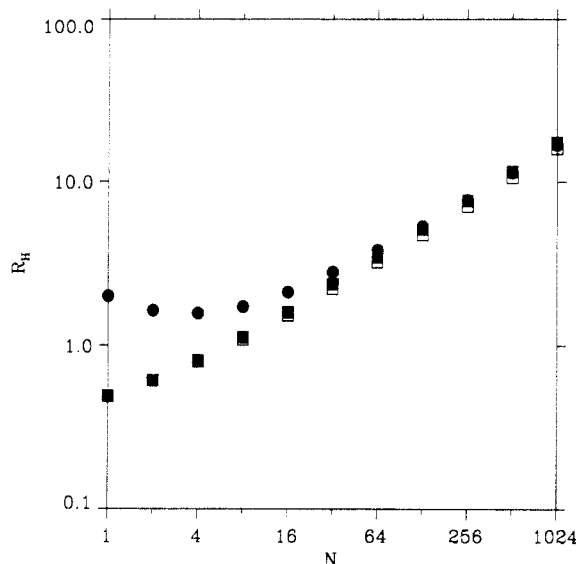


**Figure 4.** Hydrodynamic radii  $R_I$ ,  $R_K$ , and  $R_Z$  computed from the inverse radius (solid circles), from the Kirkwood approximation (open squares), and from the Zimm approximation (solid squares).

**Table I**  
Chain Size as a Function of Chain Length for  $\sigma = 0.65$  and  $a_H = 0.325^a$

$N$	$R_G$	$R_I$	$R_Z$	$N$	$R_G$	$R_I$	$R_Z$
1	0.5	2.0	0.491	64	4.71	3.82	3.46
2	0.685	1.635	0.614	128	7.00	5.35	5.12
4	0.963	1.576	0.814	256	10.74	7.72	7.65
8	1.390	1.729	1.126	512	16.40	11.33	11.5
16	2.062	2.115	1.60	1024	24.9	16.74	17.3
32	3.15	2.80	2.36				

<sup>a</sup> The statistical errors in the gyration radius  $R_G$  and inverse radius  $R_I$  are about 0.6 and 0.3%, respectively, independent of chain length. The statistical errors in the Zimm bound  $R_Z$  are about 1%, except for the  $N = 1024$  chain when they are about 1.5%.

completeness. The Zimm bound was only computed for 100 chain configurations, consequently the statistical errors are somewhat larger. To compensate for this, we used the fact that the fluctuations in  $R_Z$  and  $R_I$  are correlated, so that the ratio  $R_Z/R_I$  has a smaller variance than  $R_Z$  or  $R_I$ . Thus we have two estimates of  $R_Z$

$$\langle R_Z \rangle_{100} \text{ and } \langle R_Z/R_I \rangle_{100} \langle R_I \rangle_{1000}$$

the reported result is an average of the two estimates, weighted by the inverse of the variance of each estimate. The ratio  $R_Z/R_K$  asymptotes to a value of about 1.09 for long chains, very similar to previous results for Gaussian chains.<sup>20</sup> Again the hydrodynamic radius reaches its asymptotic value much more slowly than the gyration radius; over the range of chain lengths  $8 \leq N \leq 1024$  (i.e., a molecular weight range of  $10^4$ – $10^6$ ) the best least-squares exponents are 0.555 for  $R_K$  and 0.565 for  $R_Z$ , still consid-

erably less than that for the radius of gyration over the same molecular-weight range. The effective exponent is also dependent on the monomer friction coefficient; for smaller monomer friction (larger  $a_H$ ) the effective exponent decreases and vice versa.

There is an important caveat to our conclusion that the swelling of the internal segments of an excluded-volume chain is essentially independent of segment length; we have assumed that varying solvent conditions can be accounted for by changing the excluded volume. It would be of great interest to repeat these calculations in the presence of solvent molecules or attractive forces between the beads, to see if the same homogeneous swelling of the internal segments is observed: the CBMC method can be straightforwardly modified for these purposes. At this point we can only conclude that blob formation is not necessary to explain the slow approach of  $\nu_H$  to its asymptotic value.

**Acknowledgment.** We acknowledge helpful suggestions from one of the reviewers and from Professor Marshall Fixman (Colorado State University). This work was partially supported by the U.S. Department of Energy and Lawrence Livermore National Laboratory under Contract No. W-7405-Eng-48. The work of the FOM Institute for Atomic and Molecular Physics is part of the research program of FOM and is supported by the "Nederlandse Organisatie voor Zuiver Wetenschappelijk Onderzoek".

## References and Notes

- (1) de Gennes, P.-G. *Scaling Concepts in Polymer Physics*; Cornell University Press: Ithaca, NY, 1991.
- (2) Doi, M.; Edwards, S. F. *The Theory of Polymer Dynamics*; Oxford University Press: Oxford, U.K., 1986.
- (3) Miyaki, Y.; Einaga, Y.; Fujita, H. *Macromolecules* **1978**, *11*, 1180.
- (4) Le Guillou, J. C.; Zinn-Justin, J. *Phys. Rev. Lett.* **1977**, *39*, 95.
- (5) Akcasu, A. Z.; Han, C. C. *Macromolecules* **1979**, *12*, 276.
- (6) Nemoto, N.; Makita, Y.; Tsunashima, Y.; Kurata, M. *Macromolecules* **1984**, *17*, 425.
- (7) Weill, G.; des Cloizeaux, J. *J. Phys.* **1979**, *40*, 99.
- (8) Frenkel, D.; Mooij, G. C. A. M.; Smit, B. *J. Phys.: Condens. Matter*, **1992**, *4*, 3035.
- (9) Rosenbluth, M. N.; Rosenbluth, A. W. *J. Chem. Phys.* **1955**, *23*, 356.
- (10) Siepmann, J. I.; Frenkel, D. *Mol. Phys.* **1992**, *75*, 59.
- (11) Harris, J.; Rice, S. A. *J. Chem. Phys.* **1988**, *88*, 1298.
- (12) Frenkel, D. *Computer Simulations of Liquid Crystals*; Luckhurst, G. R., Ed.; Kluwer Academic Publishers: Dordrecht, The Netherlands, in press.
- (13) Kremer, K.; Binder, K. *Comput. Phys. Rep.* **1988**, *7*, 259.
- (14) Yamakawa, H. *Annu. Rev. Phys. Chem.* **1984**, *35*, 23.
- (15) Matsushita, Y.; Noda, I.; Nagasawa, M.; Lodge, T. P.; Amis, E. J.; Han, C. C. *Macromolecules* **1984**, *17*, 1785.
- (16) Guttman, C. M. *J. Stat. Phys.* **1984**, *36*, 717.
- (17) Zimm, B. H. *Macromolecules* **1980**, *13*, 592.
- (18) Rey, A.; Freire, J. J.; Garcia de la Torre, J. *Macromolecules* **1987**, *20*, 342.
- (19) Fixman, M. *J. Chem. Phys.* **1983**, *78*, 1588.
- (20) Fixman, M. *J. Chem. Phys.* **1983**, *78*, 1594.
- (21) Rotne, J.; Prager, S. *J. Chem. Phys.* **1969**, *50*, 4831.